J. Earth Syst. Sci. (2022)131 239
https://doi.org/10.1007/s12040-022-01984-0

Moment tensor solutions of some regional events using 3-component single station waveform data

Rohtash Kumar[1,*], Arjun Kumar[2], S C Gupta[3], S P Singh[4], Rajeev Saran Ahluwalia[5] and Raghav Singh[1]

[1]*Department of Geophysics, Institute of Science, Banaras Hindu University, Varanasi, UP 221 005, India.*
[2]*Department of Civil Engineering, Arni University, Kathgarh, Himachal Pradesh 176 401, India.*
[3]*Department of Earthquake Engineering, Indian Institute of Technology, Roorkee, Uttarakhand 247 667, India.*
[4]*Department of Atomic Energy, Mumbai, India.*
[5]*Centre for Glaciology, Wadia Institute of Himalayan Geology, Dehradun, Uttarakhand, India.*
**Corresponding author. e-mail: rohtash21@bhu.ac.in*

MS received 11 February 2020; revised 19 September 2020; accepted 17 June 2022

The information about the ongoing tectonic faulting process causing earthquakes in an area having single or sparse seismological waveform data available remains a mystery for seismologists. The usual P-wave polarity inversion is unable to find the solution to the earthquake mechanism if the event is recorded with a lower azimuthal coverage network. Recently some seismologists seek towards the moment tensor solution and tried to find the focal mechanisms of earthquakes. The present work is a step in the same direction. Twelve regional earthquakes recorded by a distant seismological network in the Siang region of Arunachal Himalaya have been analyzed using ISOLA codes developed by Sokos and Zahradnik (2008). The solutions obtained by CMT Harvard by inversion of a large number of available waveform data have been considered standards. In the present study, moment tensor solutions have been estimated using the hypocentre locations given by the CMT catalog. The obtained solutions are comparable with the CMT solutions reported. High variance reduction has been obtained for the analyzed earthquakes that agree with the observations by Delouis and Legrand (1999), Kim and Kraeva (1999), Kim *et al.* (2000), Dragger (2003), and Maercklin *et al.* (2011) that moment tensor solutions can be obtained by using single station waveform data. The present study infers that the moment tensor inversion would be useful for obtaining information about the ongoing faulting process for which limited waveform data is available. For most of the Himalayan earthquakes which occur northern side of the Main Central Thrust (MCT), the seismological networks in those areas are either very sparse or not instrumented at all. The knowledge of undergone tectonics of this region was established with various faults visible on the surface by geologists and lacks the knowledge of the present situation of ongoing tectonics of the region. Hence, the moment tensor solutions obtained using available data will help in understanding the ongoing tectonic processes of the regions lacking well coverage of seismological networks.

Keywords. Moment tensor; ISOLA; CMT Harvard; single station; Himalaya.

Published online: 19 November 2022

1. Introduction

In the last two decades, there is a great evolution in the understanding of the earthquake source process as a result of technology development. In an area, to understand the tectonic processes and the assessment of expected deformation and damage patterns, the determination of the focal mechanism is very important (Delouis and Legrand 1999). The inversion of first motion polarity is well known for focal mechanism determination. This method provides a very good solution for earthquakes that occurred within the network and has well coverage of seismic stations. However, this method is very much constrained as it requires a good azimuthal coverage of earthquake records. Hence, does not work properly when the stations recording data are unevenly distributed or the source lies outside the network. For most of the Higher Himalayan earthquakes, the seismological networks are either very sparse or not instrumented at all. Hence, it is almost impossible to estimate the focal mechanism solution for these earthquakes using earlier methods. Furthermore, there is almost no seismological data exchange between India and China so the estimation of the focal mechanism for these earthquakes is not possible either by Chinese or Indian data. In such cases, the researchers are left only with the alternatives to obtain the solutions with limited recorded waveform data.

The waveform inversion technique is very popular to estimate source mechanism using multi-station data (Zahradnik *et al.* 2008) and some researchers demonstrated that the focal mechanism solution can also be obtained even with a single station waveform data (Langston 1981; Dreger and Helmberger 1991; Kim and Kraeva 1999). The single station waveform inversion has been theoretically well explained by Dreger and Helmberger (1993) and Pinar *et al.* (2003). The various sensitivity test carried out by Dreger and Helmberger (1993) suggest that 3-component single station waveform data is adequate for waveform inversion. However, more confidence in obtained results is obtained by multi-station data. The waveform data recorded at regional distances (1°– 12°) are relatively more complicated, however, the long-period Pn waves are relatively stable (Helmberger and Engen 1980) and have proven to be quite successful in source inversions (Wallace *et al.* 1981). The surface waves are more sensitive to lateral heterogeneity and shallow crustal structure (Ho-Liu *et al.* 1988; Stead 1990), so accurate knowledge of velocity and Q is needed, especially when inverted using only single station data (Walter 1993). The surface and body waves are important in the modal calibration (Pasyanos *et al.* 1996). The inversion results did not degrade by the horizontal mislocation of up to 15 km for the Baja event (Dreger 1993) and also found that good azimuthal coverage is not required when the data used is recorded on a three-component seismogram.

In the present study, an attempt has been made with a fair degree of precision, to estimate the MT solutions for 12 regional earthquakes recorded by a distant seismological network in the Siang region of Arunachal Lesser Himalaya (table 1) by waveform inversion using a 3-component single station data and ISOLA software. The solutions given by CMT Harvard are compared with obtained solutions to check their reliability.

2. Seismotectonics of the study region

The Himalaya is the highest surface feature on the planet Earth which is evolved by the collision of the Indian plate with the Eurasian plate about 50 m.y. ago. It extended between Kashmir (India) in the west and Arunachal Pradesh in the northeast and the border between India and Tibet. Himalaya structurally (tectonically) from north to south can be divided into Tibetan Himalaya (Northwest part of Arunachal Himalaya bordering Bhutan and Tibet, NE–SW trending), Higher Himalaya (limits between Tibetan Himalaya and MCT, ENE–WSW trend adjacent to Bhutan and changes to NE–SW eastward), Lesser Himalaya (limits between Higher Himalaya and Sub Himalaya, trending E–W in the western part, swing NNE–SSE till the syntaxial then NW–SE), Sub Himalaya (trending E–W near Bhutan, swings ENE–WSW towards east) and the division from east to west: The Eastern Himalaya, Central Himalaya and Western Himalaya (e.g., Gansser 1964; Le Fort 1975). The Main Himalayan Seismic belt (MHSB) is defined between MCT and MBT (Kayal 2007). Most of the highest magnitude earthquakes occurred in this belt (Kayal 2001). The Himalayan arc in the southeast joints the Burma–Andaman–Sumatra–Sunda. So the total length of the Himalayan arc is ∼5500 km which defines the boundary between Indo-Australian and Eurasian plates from Myanmar (Burma) to Sumatra and Java to Australia (Curray *et al.* 1979). Figure 1 depicts the topographic map

Table 1. *Site characteristics and geographical locations of the recording stations.*

Sl. no.	Name of station	Station code	Lat. (°N)	Long. (°E)	Elev. (mts.)	Type of soil/rock
1	Adi-Pasi	ADI	28.36°	95.26°	997	Reddish sandstone with shale
2	Ahali-Suru	AHO	28.24°	95.54°	571	Quartzite
3	Ayeng	AYE	28.15°	95.36°	272	Boulder bed
4	Ledum	LED	27.96°	95.13°	385	Boulder bed
5	Rotung	ROT	28.14°	95.16°	410	Quartzite
6	Yeksi	YEK	28.24°	94.98°	401	Conglomerate

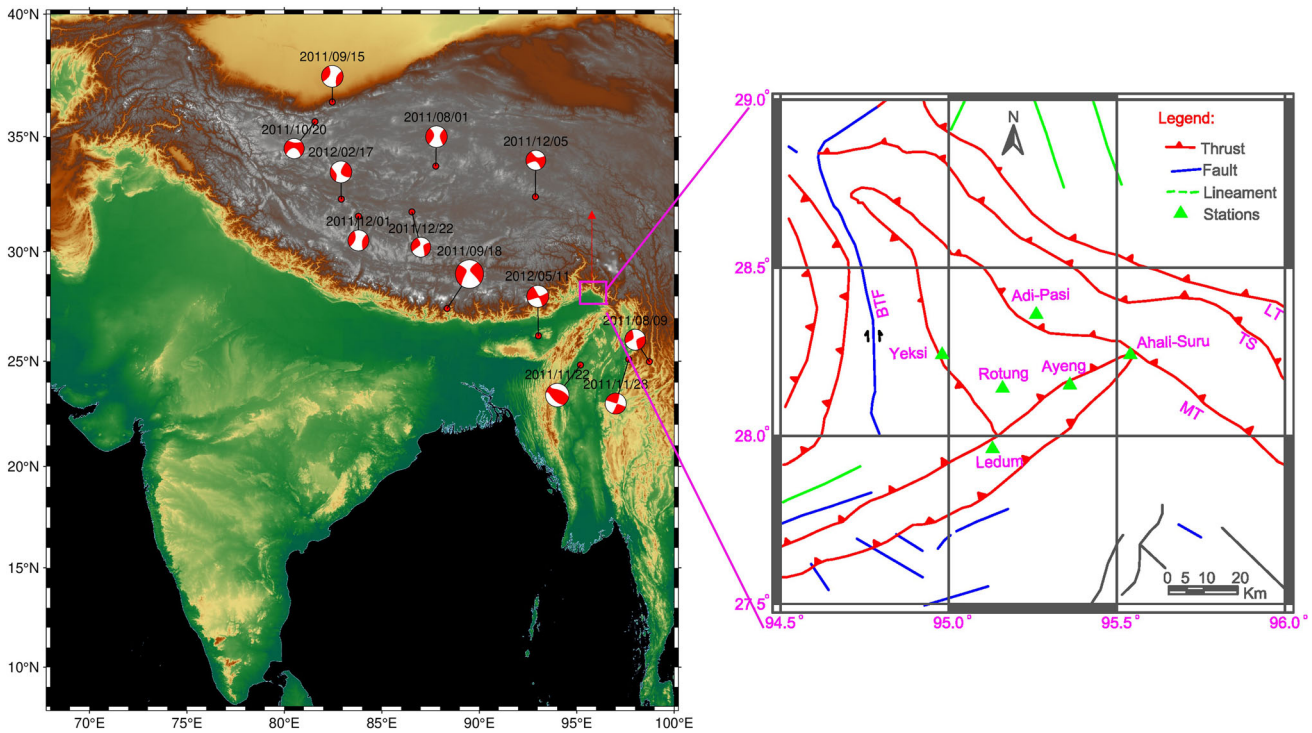

Figure 1. Map showing the hypocentral locations of earthquakes. The square box shows the location of the seismological network. (Tectonics after GSI 2010).

and the major tectonic fronts of the Indian plate on the north edge along the Himalaya, i.e., Hazara Arc, Himalayan Arc, and Burmese Arc (Kumar *et al.* 2014).

The northern part of the Himalaya consists of a tectonic belt of plate boundary and active tectonic characteristics such as the intraplate fault block regions. The tectonic belt at the plate boundary mainly consists of Himalayan tectonic features. In the northern dipping side of the Himalaya, F2 faults are also developed along with the main features. The southern boundary of the central Xizang extension region is a normal fault that represents a boundary between the Himalayan Mountains and South Xizang Plateau. The tectonic boundary is between Philippine Sea plate and Eurasian plate called Taiwan active tectonic belt. In this belt, a series of east-dipping imbricate active thrust faults and active folds were formed on the western slope and western piedmont of the central mountain range. The intraplate deformation is caused by the continuous movement of the Indian plate which is colliding with the Eurasian plate and forms the Qinghai–Xizang fault block region. There is a dispersed distribution of strong earthquakes which are running through the Qinling Range along the eastern boundary of the Qinghai–Xizang fault block region. This zone consists of some discontinuous NE- and NW-trending faults. A strongly active zone lies in the southern part of the Qinghai–Xizang fault block region called the Sichuan–Yunnan fault block. In the far north of the Tibetan

plateau, the relatively less active zone called the Xinjiang fault block region is located in the region of Cenozoic rejuvenated orogenic belt compression–depression basins, thrust faults, and active folds in the continental interior of the compressional environment (Qidong and Jianwei 2003). Nearby this zone there is the North China fault block region which is characterized mainly by graben and semi-graben basins controlled by normal faults or normal strike–slip faults. Along with all these features, China consists of small-scale features.

The Burma plate is a small tectonic or micro-plate located in Southeast Asia and is often considered a part of the Eurasian plate. It is one of the most active plates in the world as earthquakes cause a significant hazard. There is a right-lateral convergent plate boundary between Myanmar (Burma) and the Indian Ocean. The Sunda Megha thrust causes the eastward subduction along the entire plate boundary. Sumatra in the south to Myanmar in the north, the plate is occupied by various strike–slip faults. Along the 2000-km length of Sumatra, the Sumatran fault accommodates most of the right-lateral component of oblique convergence (Fitch 1972; Sieh and Natawidjaja 2000; Chlieh *et al.* 2007; McCaffrey 2009; Wang *et al.* 2014). A large component of strike slips causes the deformation beneath the Andaman Sea and is carried by an en-echelon spreading centre (Curray 2005). Another important tectonic feature is the Sagaing fault which broadly divides the country into a western half moving north with the Indian plate and an eastern half attached to the Eurasian plate. The Burma plate is lying between the Indian plate and the Sagaing fault (Curray *et al.* 1979). A terrene which includes the Shan Plateau is between the Sagaing fault and Sunda blocks.

3. Methodology

The moment tensor can be estimated by the inversion of the regional seismogram and assuming the spatial and temporal point source (Dreger 2003) as in equation (1);

$$U_k(x,t) = M_{ij}(\xi, t{-}\tau) \times G_{ki,j}(x,z,t), \quad (1)$$

Here, at spatial coordinate location x, $U_k(x, t)$ is the recorded seismogram of the kth component of ground velocity; $G_{ki,j}(x, z, t)$ is the spatial derivative of Green's function and Green's function is the impulse response of the ground at location c and time t. the Double couple force strength is described by the seismic moment tensor $M_{ij}(\xi, t{-}\tau)$; i and j are the indices of geographical direction and ξ is the position vector of a point source with coordinates ξ_1, ξ_2, ξ_3 for the north, east and down, respectively.

Herrmann and Wang (1985) showed that at a free surface, the Fourier transformed displacement of the three components of recorded seismogram due to arbitrary oriented double couple without moment can be represented as after Chang *et al.* (2011):

$$U_z = A_1 \cdot \mathrm{ZSS} + A_2 \cdot \mathrm{ZDS} + A_3 \cdot \mathrm{ZDD}, \quad (2)$$

$$U_R = A_1 \cdot \mathrm{RSS} + A_2 \cdot \mathrm{RDS} + A_3 \cdot \mathrm{RDD}, \quad (3)$$

$$U_T = A_4 \cdot \mathrm{TSS} + A_5 \cdot \mathrm{TDS}. \quad (4)$$

Here, U_z, U_R, U_T are the vertical displacement, radial replacement and transverse displacement, respectively. In horizontal layer earth, the ten Green functions required to calculate the wave field at an arbitrary point due to buried explosive source are denoted as ZSS, ZDS, ZDD, RSS, RDS, RDD, TSS and TDS along with ZEP and REP. For a deviatoric source the function A_i can be estimated as:

$$A_1 = \frac{1}{2}\left(M_{xx} - M_{yy}\right)\cos(2az) + M_{xy}\sin(2az), \quad (5)$$

$$A_2 = M_{xz}\cos(az) + M_{yz}\sin(az), \quad (6)$$

$$A_3 = -\frac{1}{2}\left(M_{xx} + M_{yy}\right), \quad (7)$$

$$A_4 = \frac{1}{2}\left(M_{xx} - M_{yy}\right)\sin(2az) - M_{xy}\cos(2az), \quad (8)$$

$$A_5 = -M_{yz}\cos(az) + M_{xz}\sin(az). \quad (9)$$

Table 2. *Velocity model for the Lower Siang Region (Khattri et al. 1983).*

Depth (km)	V_p (km/s)	V_s (km/s)	ρ (g/cm^3)
0	3.00	1.734	2.300
1	5.20	3.006	2.740
5	5.20	3.006	2.740
10	5.20	3.006	2.740
16	6.00	3.468	2.900
20	6.00	3.468	2.900
30	6.00	3.468	2.900
45	7.91	4.572	3.282

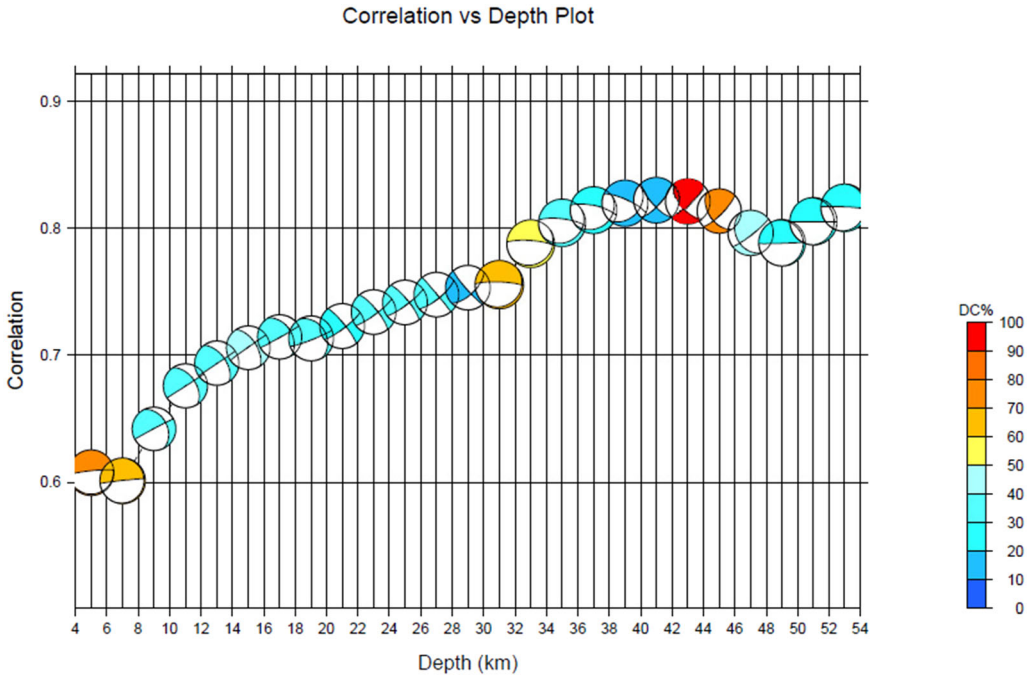

Figure 2. The correlation between observed and synthetic waveforms and the focal mechanism solutions of Sikkim earthquake obtained at various trial depths by the vertical grid search method. The colours of the beach balls represent DC%.

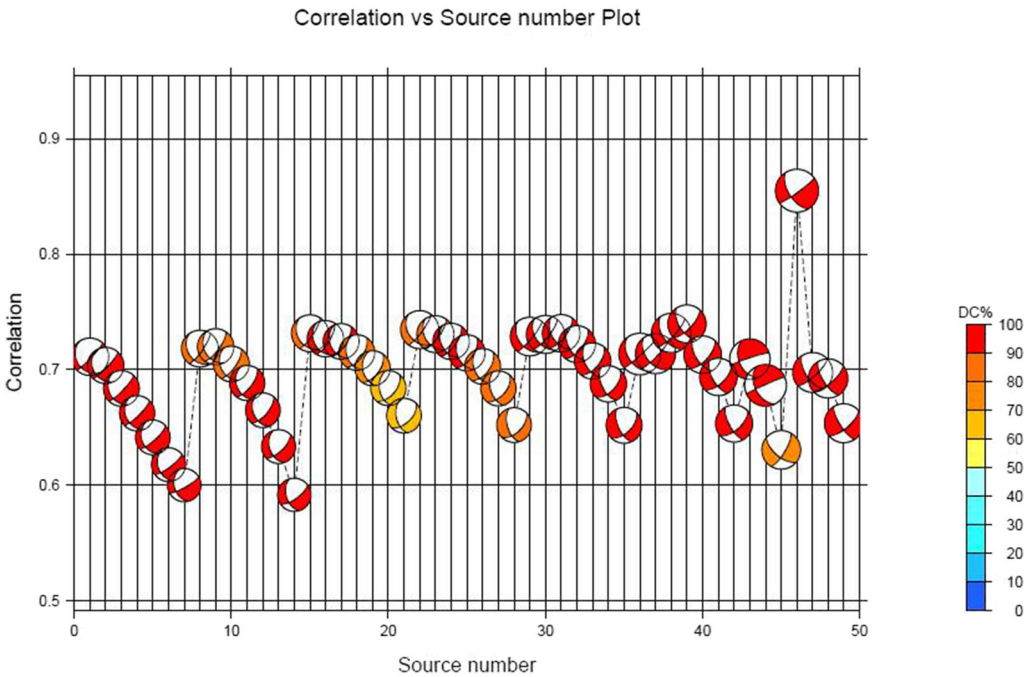

Figure 3. The correlation between observed and synthetic waveforms is shown by contours of different colours and focal mechanism solutions of Sikkim earthquakes obtained at various trials of 49-point sources on a 2×2 km^2 a grid along with NS and EW directions. The colours of the beach balls represent DC%.

Here *az* represents the source-receiver azimuth. The moment tensor (M_{ij}) consists of isotropic ($M^{\text{isotropic}}$) and a deviatoric ($M^{\text{deviatoric}}$) part in which deviatoric ($M^{\text{deviatoric}}$) can be further decomposed into double-couple (M^{DC}) and a compensated linear vector dipole (M^{CLVD}) (Bormann 2009). The isotropic component of the moment (i.e., volume change in the source) can be explained by the eigenvalues of the moment tensor. The isotropic component represents an explosion

Table 3. *Data used for the estimation of moment tensor solutions CMT Harvard (Global Centroid Moment Tensor Catalogue).*

			Data used for inversion					
			Body-waves		Mental-waves		Surface-waves	
Location name	Date yyyy/mm/dd	Time hh:mm:ss	Stations	Components	Stations	Components	Stations	Components
Xizang	2011/08/01	19:40:55	68	94	0	0	116	212
Myanmar–China Border	2011/08/09	11:50:20	58	67	0	0	113	119
Southern Xinjiang, China	2011/09/15	15:27:04	71	106	0	0	100	186
Sikkim, India	2011/09/18	12:40:59	145	338	141	314	151	367
Southern Xinjiang, China	2011/10/20	20:52:40	24	28	0	0	76	114
Myanmar	2011/11/21	03:15:42	134	252	52	54	150	318
Myanmar–China Border	2011/11/28	15:06:49	47	55	0	0	110	190
Xizang	2011/12/01	03:50:59	56	73	0	0	101	170
Xizang	2011/12/05	18:55:45	18	19	0	0	71	100
Xizang	2011/12/22	23:42:57	13	13	0	0	66	88
Northeastern India	2012/05/11	12:41:37	87	127	0	0	127	214
Xizang	2012/02/17	15:44:25	91	136	0	0	127	232

Table 4. *Hypocentral parameters and moment tensor solutions estimated by CMT Harvard (Global Centroid Moment Tensor Catalogue).*

Location name	Lat. (°N)	Long. (°E)	Date	Time	Depth (km)	M_w	NP1 strike	NP1 dip	NP1 rake	NP2 strike	NP2 dip	NP2 rake
Xizang	33.75	87.77	2011/08/01	19:40:55	21.8	5.3	319	81	–177	229	87	–9
Myanmar–China Border	24.98	98.73	2011/08/09	11:50:20	20.1	5.1	251	86	1	161	89	176
Southern Xinjiang, China	36.45	82.46	2011/09/15	15:27:04	12.0	5.3	335	82	–179	245	89	–8
Sikkim, India	27.44	88.35	2011/09/18	12:40:59	46	6.9	216	72	–16	310	79	–162
Southern Xinjiang, China	35.63	81.57	2011/10/20	20:52:40	24.0	5.0	228	72	–19	324	72	–161
Myanmar	24.82	95.19	2011/11/21	03:15:42	129	5.8	143	48	118	284	49	62
Myanmar–China Border	25.09	97.67	2011/11/28	15:06:50	17.6	5.2	20	81	–177	289	87	–9
Xizang	31.57	83.80	2011/12/01	03:50:59	22.0	5.1	329	84	–176	239	86	–6
Xizang	32.42	92.88	2011/12/05	18:55:45	28.5	4.9	333	82	–177	243	87	–8
Xizang	31.76	86.54	2011/12/22	23:42:57	26.1	4.9	337	75	–169	244	79	–15
Northeastern India	26.18	93.03	2012/05/11	12:41:37	46.1	5.4	67	83	7	336	84	173
Xizang	32.32	82.92	2012/02/17	15:44:25	20.9	5.4	118	70	172	210	83	20

or the source has an implosive component and can be explained by the sum of eigenvalues positive or negative, respectively. If the sum of eigenvalues is zero then the moment tensor has only deviatoric components. If one of the eigenvalues is zero, the deviatoric ($M^{\text{deviatoric}}$) is a pure double couple (M^{DC}). The moment can be decomposed into a major and minor double couple (Kanamori and Given 1981), or a double couple and a compensated linear vector dipole (CLVD) or M^{CLVD} (Knopoff and Randall 1970; Jost and Herrmann 1989), if the sum of the eigenvalue is zero. While each individual eigenvalue is non-zero, a CLVD represents the seismic sources having no volume change, net force, or net moment. The reliability of the obtained solution is estimated by the variance reduction (VR) given by Dreger (2003);

$$VR = \left[1 - \sum \sqrt{\frac{(d_i - s_i)^2}{{d_i}^2}}\right]. \qquad (10)$$

Here d_i and s_i are the observed and synthetic data, respectively.

Table 5. *Moment tensor inversion using single station three component data.*

Location name	Magnitude M_w	NP1 strike	NP1 dip	NP1 rake	NP2 strike	NP2 dip	NP2 rake	DC %	CLVD %	*P*-axis azimuth	*P*-axis plunge	*T*-axis azimuth	*T*-axis plunge	Correlation	Epicentre distance (km)
Xizang	5.5	337	86	–175	66	85	–4			22	6	112	1	0.73	1037.5
Myanmar–China Border	5.1	244	65	12	149	79	155	69.7	30.3	198	9	284	25	0.91	510.5
Southern Xinjiang, China	5.4	170	81	–173	79	83	–9	77	23	214	11	305	1	0.78	985.4
Sikkim, India	7.1	208	74	–16	303	75	–163	77.3	22.7	165	22	75	1	0.76	775.0
Southern Xinjiang, China	4.9	71	88	–11	161	79	–178	88.9	11.1	206	9	117	6	0.64	1725.7
Myanmar	6.1	296	56	108	266	38	65	81.6	18.6	13	9	253	72	0.76	366.7
Myanmar–China Border	5.0	6	82	–176	275	86	–8			50	9	141	2	0.61	1139.8
Xizang	5.3	333	85	–176	62	86	–6	87.4	12.6	18	6	108	1	0.72	1326.1
Xizang	4.9	351	81	–176	260	86	–9	66.7	33.3	35	9	125	3	0.68	543.2
Xizang	5.0	124	86	–172	33	82	–4	50.6	49.4	169	8	258	3	0.62	1032.5
Northeastern India	5.4	73	83	3	162	87	173	91.3	8.7	208	3	117	7	0.64	335.6
Xizang	5.3	292	63	177	203	87	27	66.6	33.4	334	17	71	20	0.78	1443.2

4. Result and discussion

The moment tensor retrieval technique is most popular for multi-station data; however, some researchers earlier tried to obtain the solution using single-station data. In the present study, an attempt has been made with a fair degree of precession, to estimate the MT solutions of some events with known solutions reported by CMT Harvard by using single-station data recorded on a local network (table 1) deployed in the Siang region of Arunachal Himalaya. The ISOLA software developed by Sokos and Zahradnik (2008) has been used for analysis. It is based on six elementary MTs and by minimizing the difference between the observed and synthetic displacement in the least square sense at a set of predefined trial source positions and trial origin times.

The general procedure for hypocentral location determination using the ISOLA software is a step-by-step process. The velocity model given by Khattri *et al.* (1983) shown in table 2 has been used for the computation of Green's function. The depth of the source can be determined by the vertical grid search by fixing the epicentre position. The optimum source depth is found by performing the inversion at several depths. The Green's function is a function of time hence the depth. So the observed seismogram is also a function of depth. A vertical grid search provides a single depth corresponding to the highest correlation and DC% (figure 2). At a particular depth estimated by the trial method, we seek the centroid in the horizontal plane, using 49 point stencils, 14 km NS and 14 km EW grids in 2×2 km steps (figure 3). Grid search provides a new optimum epicentre location, corresponding to the best correlation and improves the centroid position for a particular depth (table 3). Also, there is no change in the results with further refinement in the grid in NS and EW directions. The final MTs can be obtained by performing inversion using the final position of the source.

The CMT Harvard estimates the MTs of most of the earthquakes that occurred worldwide using data from multiple stations. So the solution given by CMT Harvard has been considered standard and used for comparing the results obtained. The three basic parameters are required as priory information for moment tensor inversion; structural velocity model, hypocentre location and the frequency band used for inversion. The earthquakes analyzed in the present study are distant

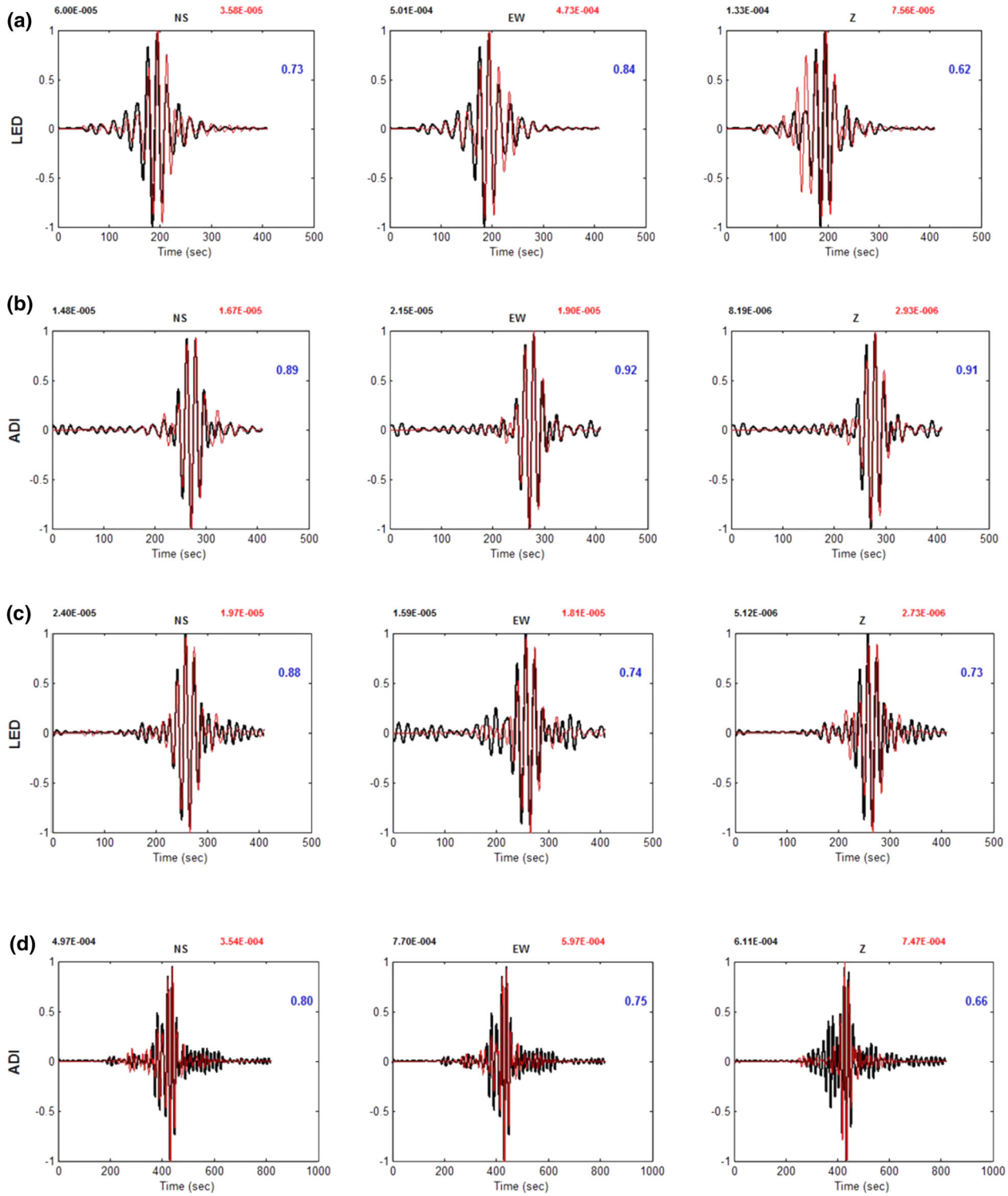

Figure 4. Plot showing comparisons between observed (black) and synthetic waveforms (red) (**a**) Xizang (2011/08/01), (**b**) Myanmar–China Border (2011/08/09), (**c**) Sikkim, India (2011/09/18), (**d**) Southern Xinjiang, China (2011/10/20), (**e**) Myanmar (2011/11/21), (**f**) Myanmar–China Border (2011/11/28), (**g**) Xizang (2011/12/01). The Black waveform and red waveform represent observed and synthetic waveforms, respectively, while the blue colour number represents the variance reduction (VR) between the waveforms.

from the seismological network, so the estimation of good hypocentre parameters is not possible and the hypocentral locations reported by CMT Harvard (table 3) have been adopted for analysis. Table 4 represents the solution obtained by CMT Harvard. The frequency bands to be used in

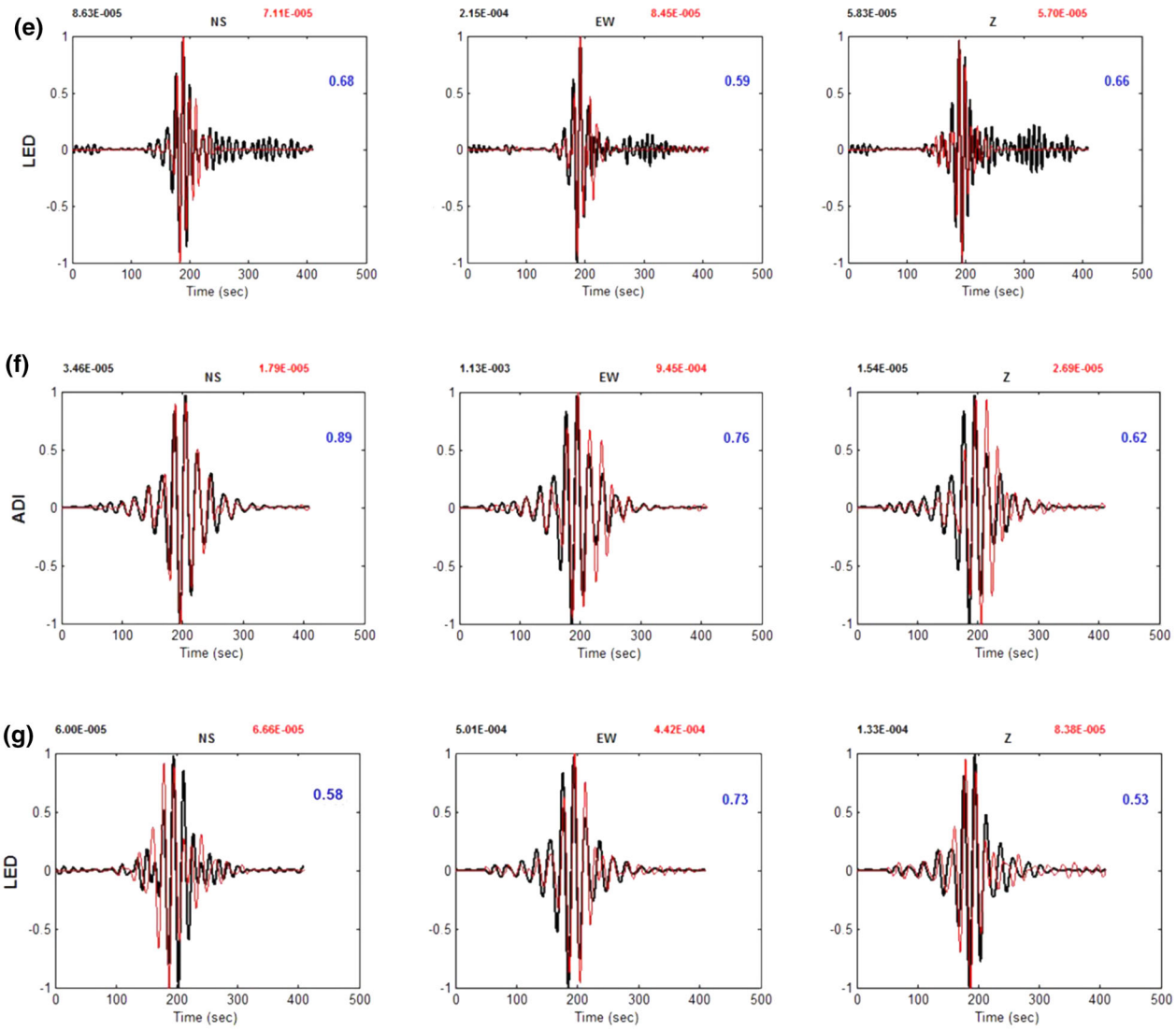

Figure 4. (*Continued.*)

inversion are obtained by using the utilities of ISOLA. The frequency bands with good S/N ratios have been used. So different frequency band has been used for different earthquake. The final results obtained from moment tensor inversion are given in table 5.

The basic parameters to explain any fault are strike, dip and rake. The estimation of the focal mechanism by any method gives two nodal planes; one (NP1) is parallel to the fault plane and another (NP2) is perpendicular to the first. Unfortunately, there is no method to discriminate between the two except the help of other geophysical methods. The nodal plane (NP1) reported by one agency may be corresponding to the nodal plane (NP2) reported by another agency. Another one is the strike of any fault which can be represented as strike = strike±180°. It means strikes 270° and 90° are representing the strike of the same fault plane. Hence the MTs estimated in the present study and reported by CMT Harvard are comparable. Figure 4(a–g) shows the correlation between observed (black coloured) and synthetic seismograms (red coloured). The variance reduction for analyzed earthquakes (VR) is quite high.

5. Conclusion

Moment tensor inversion has been performed to find the focal mechanism of 12 earthquakes recorded at regional distances by a local seismological network in the Siang region of Arunachal Himalaya. The solutions reported by CMT Harvard have been treated as standard and obtained solutions have been found comparable. Also, the

variance reduction for the analyzed earthquakes is found high. This indicates the ability of the moment tensor inversion method to get the solution even if less azimuthal data is available. This agreement with the observations by Delouis and Legrand (1999), Kim and Kraeva (1999), Dragger (2003), Kim *et al.* (2002) and Maercklin *et al.* (2011) that the focal mechanism can be obtained using single-station data.

Dreger and Helmberger (1993) and Walter (1993) show that an exact Earth's crustal model can be compensated by varying the depth or distance of the source. They also found that the best fit solution is not much affected by the small changes in the epicentre of the earthquake. The significant variation in the solution can be observed due to the oversimplification in the crustal velocity model. Hence, the most important priory information is the crustal velocity model which should be confirmed by the data as much as possible. Another important parameter is the frequency band used for inversion which can be decided by estimating the signal-to-noise ratio.

Hence, the present study concludes that waveform inversion can be applied to the near field single station data provided several parameters are carefully used. But authors are not assuring that such good solutions can be obtained in all cases as the solution is affected by three basic parameters; structural velocity model, hypocentre location and the frequency band used for inversion. Yet this method would be very useful to obtain the information about the earthquake having limited data availability, with the help of a simple finite-dimension source model. Also in a region like India where most of our stations are below the Main Central Thrust (MCT) as in this situation the azimuthal coverage may not be good. The moment tensor solutions obtained by careful waveform inversion from a few stations will help in understanding the ongoing seismo-tectonic processes in the region.

Acknowledgements

The authors are very grateful to Prof H R Wason for providing the data. The authors are also thankful to Jaypee Ventures Pvt. Ltd., Noida for funding the project under which data is collected.

Author statement

Dr Rohtash Kumar performed the inversion and wrote the manuscript. Dr Arjun Kumar formatted the waveform. Dr S C Gupta supervised the manuscript. Mr S P Singh and Dr Rajeev Saran Ahluwalia helped in improving the English and text. Mr Ragav Singh plotted the high-quality figures.

References

Chang K, Chi W C, Gung Y, Dreger D, Lee W H and Chiu H C 2011 Moment tensor inversions using strong motion waveforms of Taiwan TSMIP data, 1993–2009; *Tectonophys.* **511(1–2)** 53–66.

Chlieh M, Avouac J P, Hjorleifsdottir V, Song T R A, Ji C, Sieh K, Sladen A, Hebert H, Prawirodirdjo L, Bock Y and Galetzka J 2007 Coseismic slip and after slip of the great M_w 9.15 Sumatra–Andaman earthquake of 2004; *Bull. Seismol. Soc. Am.* **97(1A)** S152–S173.

Curray J R 2005 Tectonics and history of the Andaman Sea region; *J. Asian Earth Sci.* **25(1)** 187–232.

Curray J R, Moore D G, Lawver L A, Emmel F J, Raitt R W, Henry M and Kieckhefer R 1979 Tectonics of the Andaman Sea and Burma: Convergent margins, pp. 189–198.

Delouis B and Legrand D 1999 Focal mechanism determination and identification of the fault plane of earthquakes using only one or two near-source seismic recordings; *Bull. Seismol. Soc. Am.* **89(6)** 1558–1574.

Dreger D S 1993 Modeling earthquakes with local and regional broadband data, PhDT. Calif Inst of Tectnol, Pasadena.

Dreger D S 2003 TDMT_INV: Time domain seismic moment tensor inversion, *Int. Handbk. Earthquake Eng. Seismol*, 81p.

Dreger D S and Helmberger D V 1991 Complex faulting deduced from broadband modeling of the 28 February 1990 Upland earthquake (M_L = 5.2); *Bull. Seismol. Soc. Am.* **81(4)** 1129–1144.

Dreger D S and Helmberger D V 1993 Determination of source parameters at regional distances with three-component sparse network data; *J. Geophys. Res.: Solid Earth* **98(B5)** 8107–8125.

Fitch T J 1972 Plate convergence, transcurrent faults, and internal deformation adjacent to southeast Asia and the western Pacific; *J. Geophys. Res.* **77(23)** 4432–4460.

Gansser A 1964 Geology of the Himalayas, Interscience Publishers, John Wiley, London.

Helmberger D V and Engen G R 1980 Modeling the long-period body waves from shallow earthquakes at regional ranges; *Bull. Seismol. Soc. Am.* **70(5)** 1699–1714.

Herrmann R B and Wang C Y 1985 A comparison of synthetic seismograms; *Bull. Seismol. Soc. Am.* **75(1)** 41–56.

Ho-Liu P, Kanamori H and Clayton R W 1988 Applications of attenuation tomography to Imperial Valley and Coso-Indian Wells region, southern California; *J. Geophys. Res.: Solid Earth* **93(B9)** 10,501–10,520.

Jost M U and Herrmann R B 1989 A student's guide to and review of moment tensors; *Seismol. Res. Lett.* **60(2)** 37–57.

Kanamori H and Given J W 1981 Use of long-period surface waves for rapid determination of earthquake-source parameters; *Phys. Earth Planet. Interior.* **27(1)** 8–31.

Kayal J R 2001 Microearthquake activity in some parts of the Himalaya and the tectonic model; *Tectonophys.* **339(3–4)** 331–351.

Kayal J R 2007 Recent large earthquakes in India: Seismotectonic perspective; *IAGR Memoir* **10** 189–199.

Khattri K, Wyss M, Gaur V K, Saha S N and Bansal V K 1983 Local seismic activity in the region of the Assam gap, northeast India; *Bull. Seismol. Soc. Am.* **73(2)** 459–469.

Kim S G and Kraeva N 1999 Source parameter determination of local earthquakes in Korea using moment tensor inversion of single station data; *Bull. Seismol. Soc. Am.* **89(4)** 1077–1082.

Kim S G, Kraeva N and Chen Y T 2000 Source parameter determination of regional earthquakes in the Far East using moment tensor inversion of single-station data; *Tectonophys.* **317(1–2)** 125–136.

Kim W, Seeber L and Armbruster J G 2002 Source process of the M_w 5.0 Au Sable Forks, New York, Earthquake sequence from local aftershock monitoring network data; In: *AGU Fall Meeting Abstracts* **2002** S22D-01, 1077–1082.

Knopoff L and Randall M J 1970 The compensated linear-vector dipole: A possible mechanism for deep earthquakes; *J. Geophys. Res.* **75(26)** 4957–4963.

Kumar R, Gupta S C and Kumar A 2014 Attenuation characteristics of seismic body waves for the crust of Lower Siang region of Arunachal Himalaya; *Int. J. Adv. Res.* **2(6)** 742–755.

Langston C A 1981 Source inversion of seismic waveforms: The Koyna, India, earthquakes of 13 September 1967; *Bull. Seismol. Soc. Am.* **71(1)** 1–24.

Le Fort P 1975 Himalayas: The collided range. Present knowledge of the continental arc; *Am. J. Sci.* **275(1)** 1–44.

Maercklin N, Zollo A, Orefice A, Festa G, Emolo A, De Matteis R, Delouis B and Bobbio A 2011 The effectiveness of a distant accelerometer array to compute seismic source parameters: The April 2009 L'Aquila earthquake case history; *Bull. Seismol. Soc. Am.* **101(1)** 354–365.

McCaffrey R 2009 The tectonic framework of the Sumatran subduction zone; *Ann. Rev. Earth Planet. Sci.* **37** 345–366.

Pasyanos M E, Dreger D S and Romanowicz B 1996 Toward real-time estimation of regional moment tensors; *Bull. Seismol. Soc. Am.* **86(5)** 1255–1269.

Pinar A, Kuge K and Honkura Y 2003 Moment tensor inversion of recent small to moderate sized earthquakes: Implications for seismic hazard and active tectonics beneath the Sea of Marmara; *Geophys. J. Int.* **153(1)** 133–145.

Qidong X and Jianwei L 2003 Migration of ore-forming fluids and its relation to zoning of mineralization in northern Lanping Cu-polymetallic metallogenic area, Yunnan Province: Evidence from fluid inclusions and stable isotopes; *Miner. Deposits-Beijing* **22(4)** 375–376.

Sieh K and Natawidjaja D 2000 Neotectonics of the Sumatran fault, Indonesia; *J. Geophys. Res.: Solid Earth* **105(B12)** 28,295–28,326.

Sokos E N and Zahradnik J 2008 ISOLA a Fortran code and a Matlab GUI to perform multiple-point source inversion of seismic data; *Comp. Geosci.* **34(8)** 967–977.

Stead R J 1990 *Finite differences and a coupled analytic technique with applications to explosions and earthquakes*, Doctoral dissertation, California Institute of Technology.

Wallace T C, Helmberger D V and Mellman G R 1981 A technique for the inversion of regional data in source parameter studies. *J. Geophys. Res.: Solid Earth* **86(B3)** 1679–1685.

Walter W R 1993 Source parameters of the June 29, 1992 Little Skull Mountain earthquake from complete regional waveforms at a single station; *Geophys. Res. Lett.* **20(5)** 403–406.

Wang Y, Sieh K, Tun S T, Lai K Y and Myint T 2014 Active tectonics and earthquake potential of the Myanmar region; *J. Geophys. Res.: Solid Earth* **119(4)** 3767–3822.

Zahradnik J, Jansky J and Plicka V 2008 Detailed waveform inversion for moment tensors of $M \sim 4$ events: Examples from the Corinth Gulf, Greece; *Bull. Seismol. Soc. Am.* **98(6)** 2756–2771.

Corresponding editor: Anand Joshi